

An SEM and STM investigation of surface smoothing in 130 MeV Si-irradiated metglass MG2705M

H Narayan^{†||}, S B Samanta[‡], H M Agrawal[†], R P S Kushwaha[†], D Kanjilal[§], S K Sharma[‡] and A V Narlikar[‡]

[†] Department of Physics, GB Pant University of Agriculture and Technology, Pantnagar 26145, India

[‡] National Physical Laboratory, Dr K S Krishnan Marg, New Delhi 110012, India

[§] Nuclear Science Centre, Post Box No 10502, Aruna Asaf Ali Marg, New Delhi 110067, India

Received 24 June 1998, in final form 9 November 1998

Abstract. Metglass MG2705M foils of about 17 μm thickness were irradiated at 90 K by 130 MeV ^{28}Si ions, up to a fluence of 1.154×10^{16} ions cm^{-2} . The surface modifications induced by irradiation have been examined by scanning electron microscopy (SEM) and scanning tunnelling microscopy (STM). It has been observed that smoothing of the sample surface is evident in both SEM and STM micrographs. The SEM pictures show a decrease in the heights of the ‘hills’ and filling up of the ‘valleys’ on micrometre length scales. The STM pictures, on the other hand, show smoothing of scratchlike surface disorders at nanometre length scales. However, the electronic energy loss S_e , of 5.75 keV nm^{-1} , does not lead to detectable track diameters, in agreement with the existing results. The observations have been attributed to a large electronic energy deposition due to high fluence, and a subsequent local shear relaxation of the near surface atoms. The theory of shear flow mechanism has been extended further to explain the results.

1. Introduction

Fast heavy ions lose their energy primarily in the form of inelastic collisions (electronic energy loss, S_e) with the atoms in the first few micrometres of the target. As a result, these atoms are set into motion, even at very low irradiation temperatures. In amorphous solids, this leads to anisotropic plastic deformation if the sample thickness is much less compared to the projected range (R_p) of the ions. This ion beam induced plastic deformation (IBID) is identified as increase in sample dimensions perpendicular to the beam, and shrinking of sample dimensions parallel to the beam, at practically constant volume [1–4]. Besides these dimensional changes, the plastic flow phenomenon is also responsible for the modification of the irradiated surface.

The energy transferred through the inelastic collision process, from the fast heavy ions to the target atoms, results in rearrangement of the latter. The average electronic energy loss varies approximately as the square root of the ion energy [5]. Evidently, the maximum transfer of energy takes place at the surface of the target. This transferred energy excites the near surface atoms. Subsequent relaxations of these excited atoms result in their rearrangement and hence in the modification of the surface without detectable mass loss. Besides S_e , and the irradiation temperature T_i , these modifications have been found to be dependent upon two parameters, namely, the fluence of the ion beam (ϕt), and the angle of incidence θ of the beam with respect to the z -axis (the axis perpendicular to the sample length and width) [6].

^{||} Corresponding author. E-mail address: cbsh@gbpuat.ernet.in.

It is known that for normal incidence of the fast heavy ion beam ($\theta = 0^\circ$), surface smoothing results for lower fluences (up to 10^{14} Xe ions cm^{-2}) [6]. This smoothing process dominates for $\theta < 15^\circ$ (off-normal incidences). For $\theta \geq 20^\circ$, first the smoothing reduces to smaller length scales, then appearance of regular undulations takes over at higher fluences. The wavelengths of these undulations have been found to be independent of the type of ion, their incidence angle, starting surface topography of the target and the irradiation temperature. At still higher fluences (about 10^{15} ions cm^{-2}), surface roughening takes place [6]. Thus, there are three steps of surface modification already known: smoothing, wave-formation and roughening. These fluence and incidence angle dependent surface modifications have been successfully accounted for by the ion beam induced shear flow mechanism [6, 7]. However, Cliche *et al* have considered the momentum transfer driven directional mass transport process to be responsible for this effect [8].

Earlier studies have been confined mainly to the large electronic energy loss effects and therefore, the effects of higher fluences ($\phi t > 10^{15}$ ions cm^{-2}) with smaller electronic energy loss have not been analysed. This was so mainly because of the limitations imposed by the available instruments. For example, a typical laser profilometer has a step height resolution around 20 nm. Hence, a step height less than 20 nm as a result of smoothing ($\phi t = 10^{15}$ ions cm^{-2} , $\theta < 15^\circ$) is not detectable. Similarly, for the roughening ($\phi t > 10^{15}$ ions cm^{-2} , $\theta > 20^\circ$), amplitude spikes larger than $50 \mu\text{m}$ have been observed, and the laser profilometer fails in such cases [6]. Scanning electron microscopy (SEM) and scanning tunnelling microscopy (STM) together provide an efficient method to observe these types of surface modification.

In this paper SEM and STM results of 130 MeV ^{28}Si (charge state +9) ion irradiated metallic glass, MG2705M ($\text{Co}_{69}\text{B}_{12}\text{Si}_{12}\text{Fe}_4\text{Mo}_2\text{Ni}$) are presented together for the first time. The S_e value in this experiment was 5.75 keV nm^{-1} [9]. Higher values of electronic energy loss could not be considered because of the limitations of the accelerator. The mathematical formulation of the shear flow mechanism [6, 7] has been extended in section 3.1 to deal with a real surface, subjected to a normally incident ion beam.

2. Experiment

2.1. Specimen preparation

Metglass 2705M was procured from Goodfellow Cambridge, UK, in the form of foils of thickness about $25 \mu\text{m}$. The TRIM97 code gives a projected range, $R_p = 19.15 \mu\text{m}$, for 130 MeV ^{28}Si ions in this system [9]. Therefore, the foils were thinned down using the method of cold rolling, to a thickness of about $17 \mu\text{m}$, in order to avoid the ion implantation.

2.2. Irradiation procedure

Irradiation of the specimen was carried out at the Material Science Beam line of the Nuclear Science Centre, New Delhi. The irradiation temperature was maintained around 90 K throughout the experiment by pouring liquid nitrogen through a stainless steel tube attached to the copper block upon which the samples were mounted inside the irradiation chamber.

130 MeV ^{28}Si ions (charge state +9) beam, with a flux of about 10^{10} ions $\text{cm}^{-2} \text{ s}^{-1}$, was made incident normally upon the sample surface. The irradiation was continued until a fluence of 1.154×10^{16} ions cm^{-2} was reached.

2.3. SEM and STM

Surface morphology of the unirradiated and irradiated specimens was investigated by scanning electron microscopy (SEM) and scanning tunnelling microscopy (STM). The instrument model JSM-35CF, supplied by JEOL, Tokyo, was used for SEM. The STM was performed in air using a NanoScope II apparatus, supplied by Digital Instruments, USA. Both SEM and STM were carried out at the National Physical Laboratory, New Delhi.

3. Result and discussion

SEM were taken at different magnifications for both the unirradiated and irradiated surfaces of the MG2705M specimen (figures 1 and 2 respectively). It may be clearly observed that the narrow and shallow channels are eliminated completely and the wider and deeper channels have become shallower and narrower after irradiation. The micrographs clearly show a decrease in the heights of the 'hills' and filling up of the 'valleys', giving an effect of smoothing to

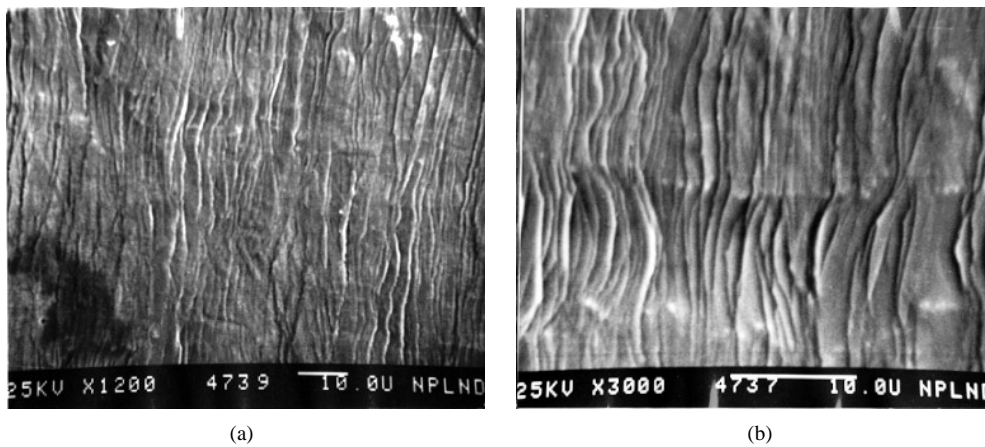


Figure 1. SEM pictures of the unirradiated metglass MG2705M.

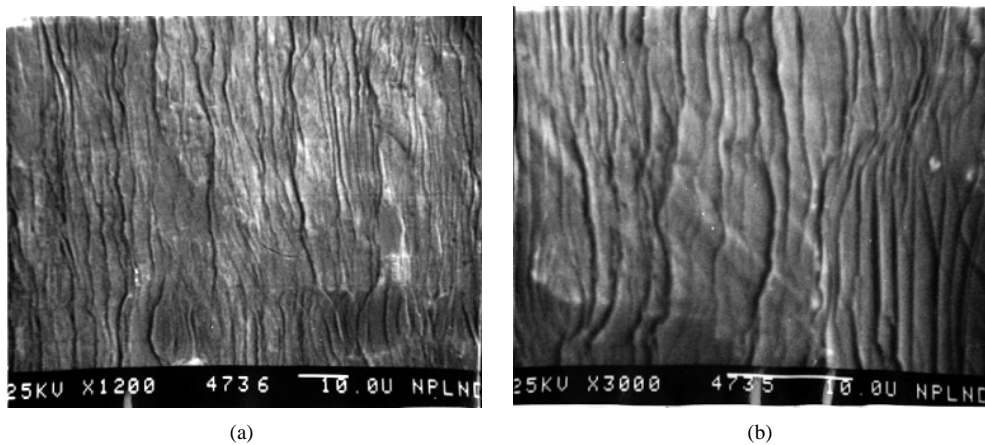
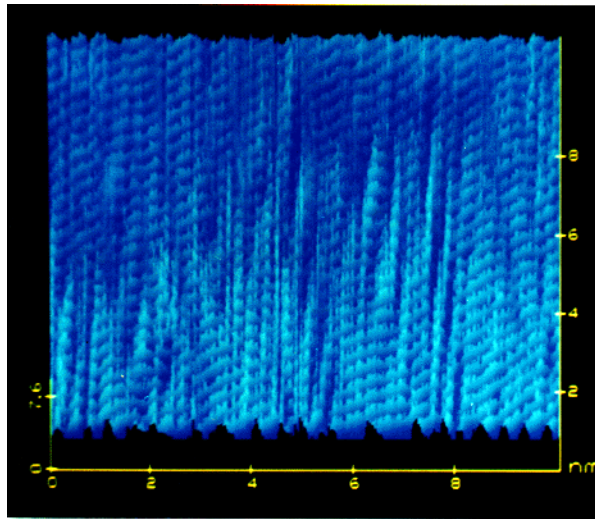
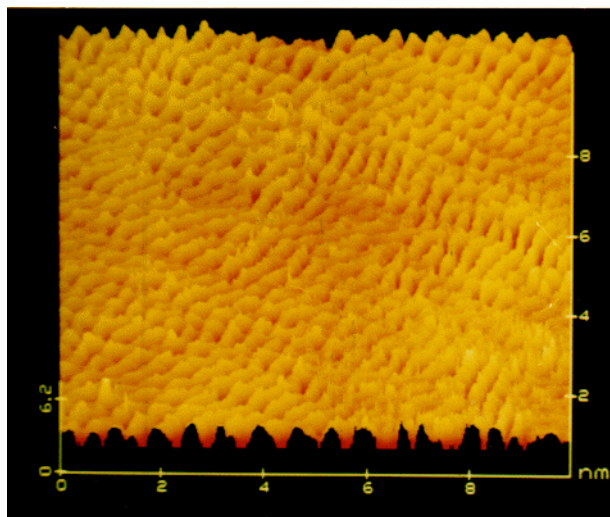


Figure 2. SEM pictures of the 130 MeV ^{28}Si ion irradiated surface of metglass MG2705M.



(a)



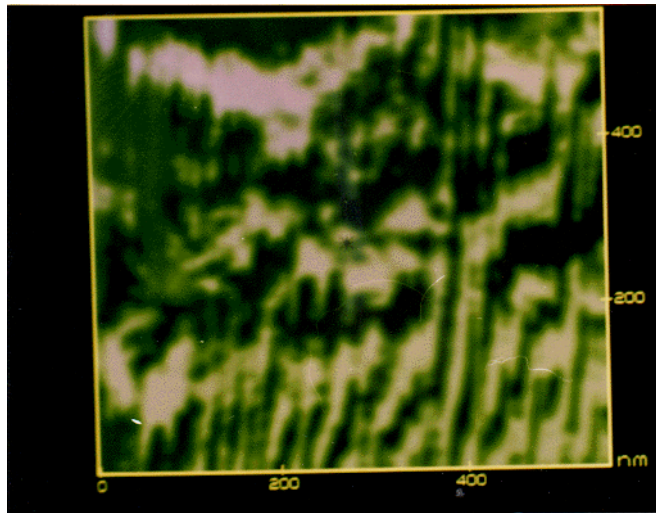
(b)

Figure 3. (a) STM picture of the unirradiated metglass MG2705M at $10 \text{ nm} \times 10 \text{ nm}$ scan area. (b) STM picture of the $130 \text{ MeV } ^{28}\text{Si}$ ion irradiated surface of metglass MG2705M at $10 \text{ nm} \times 10 \text{ nm}$ scan area.

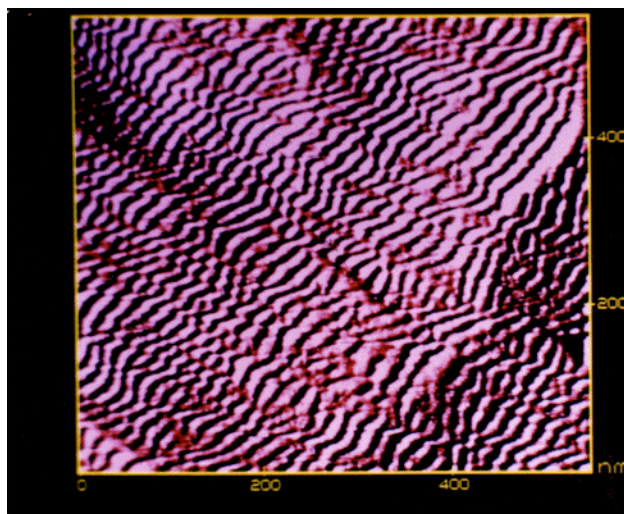
(This figure can be viewed in colour in the electronic version of the article; see <http://www.iop.org>)

the irradiated surface, as reported earlier by Guntzmann and Klaumunzer for the $\text{Fe}_{40}\text{Ni}_{40}\text{Bi}_{20}$ metallic glass and vitreous SiO_2 amorphous systems [7].

The STM of the unirradiated and irradiated specimens was carried out in order to investigate the surface modifications at smaller length scales. STM were taken for $10 \text{ nm} \times 10 \text{ nm}$, $25 \text{ nm} \times 25 \text{ nm}$ and $545 \text{ nm} \times 545 \text{ nm}$ scan areas. The STM pictures are shown in figures 3(a) and 4(a) for unirradiated and in figures 3(b) and 4(b) for irradiated specimens. The bias voltage V_b for figures 3(a) and 3(b) was -1115.4 mV , and the setpoint current I_{sp}



(a)



(b)

Figure 4. (a) STM picture of the unirradiated metglass MG2705M at $545 \text{ nm} \times 545 \text{ nm}$ scan area. (b) STM picture of the 130 MeV ^{28}Si ion irradiated surface of metglass MG2705M at $545 \text{ nm} \times 545 \text{ nm}$ scan area.

(This figure can be viewed in colour in the electronic version of the article; see <http://www.iop.org>)

was 0.07 nA for figure 3(a), and 0.14 nA for figure 3(b). Similarly, V_b was -1114.8 mV for figure (a) and -1115.4 mV for figure 4(b). The I_{sp} was 1.1 nA for figure 4(a) and 1.3 nA for figure 4(b). It is evident from figure 3(a) and (b) that sharp scratchlike disorders present in the unirradiated samples have been smoothed after irradiation. A comparison of figure 4(a) and (b) also shows a surface smoothing due to irradiation, although figure 4(a) needed more filtration. The scratchlike surface disorders result from the freezing in of surface disorders of the liquid state when the latter is rapidly quenched to form metallic glasses. All these STM

pictures show that on the smaller (nanometric) length scales, the smoothing due to heavy ion irradiation of the sample is observed as a removal or reduction of the sharp scratchlike surface disorders. However, no sign of track formation was observed in either SEM or STM pictures. This may be due to the fact that the threshold value of S_e for detectable track formation is larger [10] than that in the present work.

Recently, Audouard *et al* [11] have reported the formation of ‘hills’ and ‘hillocks’, in the GeV ion irradiated Fe₈₅B₁₅ amorphous alloy, investigated by STM. They have attributed this observation to the high electronic energy loss ($S_e > 50 \text{ keV nm}^{-1}$) of ions in the specimen. They did not observe such ‘hills’ and ‘hillocks’ for 750 MeV ⁸⁶Kr irradiation ($S_e = 19.3 \text{ keV nm}^{-1}$). In our experiment the S_e was 5.75 keV nm^{-1} , and hence the so-called ‘hills’ and ‘hillocks’ are obviously not expected. However, it is not clear from the work of Audouard *et al* whether a comparative smoothing/roughening of the 750 MeV ⁸⁶Ar irradiated surface was observed or not.

3.1. The shear flow mechanism

The observed results could be explained by the shear flow mechanism [7] within the framework of the viscoelastic model [12, 13]. This model assumes that amorphous systems behave viscoelastically under swift heavy ion irradiation. Mathematically, this can be represented by a phenomenological tensor equation [7] as follows:

$$\frac{d\varepsilon}{dt} = \frac{1}{2G} \frac{d}{dt} \left[\boldsymbol{\sigma} - \frac{\nu}{\nu+1} (\text{Tr}\boldsymbol{\sigma})\mathbf{I} \right] + \mathbf{A}_0\phi + k_0\phi \left[\boldsymbol{\sigma} - \frac{1}{3}(\text{Tr}\boldsymbol{\sigma})\mathbf{I} \right] \quad (1)$$

where G is the shear modulus and ν the Poisson number. ε , $\boldsymbol{\sigma}$ and \mathbf{I} represent the tensors of strain, stress and unity, respectively. $\text{Tr}\boldsymbol{\sigma}$ is the trace of tensor $\boldsymbol{\sigma}$. The dimension of $(k_0\phi)$ is that of fluidity and thus k_0 is related to the apparent viscosity $(2k_0\phi)^{-1}$. Thus, equation (1) combines the effects of elasticity, ion beam induced growth and viscosity together. In an irradiation experiment we consider only the ion beam induced growth and the viscosity parts, because they include the flux ϕ to give the irradiation induced effects. For stress free samples, i.e., $\boldsymbol{\sigma} = \mathbf{0}$, equation (1) is reduced to give the strain rate as $d\varepsilon/dt = \mathbf{A}_0\phi$. In the most general case, tensor \mathbf{A}_0 may be written as [7],

$$\mathbf{A}_0 = A(\delta_{ik} - 3u_i u_k) \quad i, k = x, y, z \quad (2)$$

where δ_{ik} is the Kronecker delta and \mathbf{u} (u_x, u_y, u_z) is a unit vector representing the direction of the beam.

Now we consider a swift heavy ion beam falling normally upon a real surface. There will be local variations in the direction of \mathbf{u} provided by the roughness of such surface. These variations may be taken into account by considering two effective tilt angles representing the direction of \mathbf{u} . If we take the sample surface at the $z = 0$ plane and assume that \mathbf{u} makes an angle θ with the z -axis and its projection on the $z = 0$ plane, i.e., $u \sin \theta$, makes an angle ψ with the x -axis (figure 5), then using equation (2) the tensor \mathbf{A}_0 can be written as

$$\mathbf{A}_0 = A \begin{pmatrix} 1 - 3 \sin^2 \theta \cos^2 \psi & 3 \sin^2 \theta \sin \psi \cos \psi & 3 \sin \theta \cos \theta \cos \psi \\ 3 \sin^2 \theta \sin \psi \cos \psi & 1 - 3 \sin^2 \theta \sin^2 \psi & 3 \sin \theta \cos \theta \sin \psi \\ 3 \sin \theta \cos \theta \cos \psi & 3 \sin \theta \cos \theta \sin \psi & 1 - 3 \cos^2 \theta \end{pmatrix}. \quad (3)$$

According to continuum mechanics, the expression relating strain ε to velocity \mathbf{v} is given by

$$\frac{d\varepsilon_{ik}}{dt} = \frac{1}{2} \left(\frac{\delta v_i}{\delta k} + \frac{\delta v_k}{\delta i} \right). \quad (4)$$

The equation of motion reduces to $\text{div } \boldsymbol{\sigma} = 0$ in quasi-static equilibrium. Also the relations $\boldsymbol{\sigma} = \boldsymbol{\sigma}(z)$ and $\mathbf{v} = \mathbf{v}(z)$ hold because of symmetry. Therefore, $\delta\sigma_{xz}/\delta z = \delta\sigma_{yz}/\delta z =$

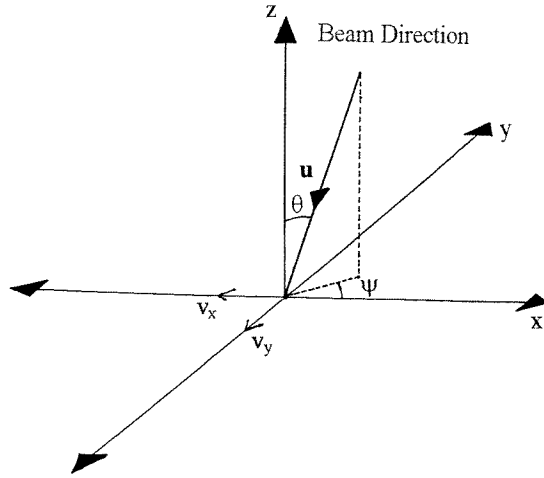


Figure 5. Schematic view of irradiation by a tilted beam. \mathbf{u} represents a unit vector along the beam direction. The sample surface is in the x - y plane. The directions of the components of shear velocity v_x and v_y are also shown.

$\delta\sigma_{zz}/\delta z = 0$, and for stress free samples at $z = 0$, this leads to $\sigma_{zz} = \sigma_{xz} = \sigma_{yz} = 0$. Using equations (3) and (4), equation (1) therefore gives the strain rate produced by irradiation as

$$\frac{d\epsilon}{dt} = A\phi \begin{pmatrix} 0 & 3 \sin^2 \theta \sin \psi \cos \psi & 3 \sin \theta \cos \theta \cos \psi \\ 3 \sin^2 \theta \sin \psi \cos \psi & 0 & 3 \sin \theta \cos \theta \sin \psi \\ 3 \sin \theta \cos \theta \cos \psi & 3 \sin \theta \cos \theta \sin \psi & 0 \end{pmatrix}. \quad (5)$$

It is noteworthy that for $\psi = 0$ equations (3) and (5) reduce to the respective tensor representations of \mathbf{A}_0 and $d\epsilon/dt$, as given by Guntzmann *et al* [6, 7].

Equating the components of equations (4) and (5) we obtain

$$\frac{d\epsilon_{xy}}{dt} = 6A\phi \sin^2 \theta \sin \psi \cos \psi \quad (6)$$

$$\frac{d\epsilon_{xz}}{dt} = 6A\phi \sin \theta \cos \theta \cos \psi \quad (7)$$

$$\frac{d\epsilon_{yz}}{dt} = 6A\phi \sin \theta \cos \theta \sin \psi \quad (8)$$

and $(d\epsilon_{xx}/dt) = (d\epsilon_{yy}/dt) = (d\epsilon_{zz}/dt) = 0$.

Equations (6) to (8) give the off-diagonal components of the strain rate. For a perfectly plane surface and normal beam incidence, $\theta = 0$, and $\psi = 0$; and hence these components of strain rate vanish. This means that no atomic motion is induced for normal irradiation of a perfectly plane surface. However, no real surface is perfectly plane. The surface disorders and irregularities of real surfaces provide non-zero values to θ and ψ . Thus $0 < \theta < \pi/2$ and $0 \leq \psi \leq 2\pi$ give non-vanishing off-diagonal components in equation (5). With these components, equations (6) to (8) give a net shear flow in the x - y plane, perpendicular to the beam direction. Evidently, this shear flow leads to surface modification.

From $(\delta v_z/\delta x) = (\delta v_z/\delta y) = 0$ and $\text{Tr}(\epsilon) = \text{div } \mathbf{v} = 0$, $\delta v_z/\delta z = 0$. Therefore, equations (7) and (8) give the shear flow in x - and y -directions at any instant as

$$(\delta v_x/\delta z) = 6A\phi \sin \theta \cos \theta \cos \psi \quad (0 < \theta < \pi/2, 0 \leq \psi \leq 2\pi) \quad (9)$$

and

$$(\delta v_y/\delta z) = 6A\phi \sin \theta \cos \theta \sin \psi \quad (0 < \theta < \pi/2, 0 \leq \psi \leq 2\pi). \quad (10)$$

Equation (9) can be integrated to give the shear velocity in the x -direction as

$$v_x = 6\phi \sin \theta \cos \theta \cos \psi \int_{-R_d \cos \theta}^0 A[S_e(z')] dz' \quad (0 < \theta < \pi/2, 0 \leq \psi \leq 2\pi) \quad (11)$$

where R_d is the deformation depth. For normal incidence of the beam, we can use the approximation $R_d \cos \theta = R_p$, the projected range of the ions in a thick target. Moreover, the surface modifications are concerned with the first few layers of the target, i.e. $z \rightarrow 0$. Therefore, the integral in equation (11) can be approximated as $R_p A_{max}$, with $A_{max} = A(S_e)_{surface}$. With this, equation (11) reduces to give the shear velocity in the x -direction as

$$v_x = 6R_p A_{max} \phi \sin \theta \cos \theta \cos \psi \quad (0 < \theta < \pi/2, 0 \leq \psi \leq 2\pi). \quad (12)$$

Similarly, from equation (10),

$$v_y = 6R_p A_{max} \phi \sin \theta \cos \theta \sin \psi \quad (0 < \theta < \pi/2, 0 \leq \psi \leq 2\pi). \quad (13)$$

Integrating with respect to time, these equations give the shifts caused by the shear velocities in total irradiation time t as

$$\Delta x = 6R_p A_{max} \Phi \sin \theta \cos \theta \cos \psi \quad (0 < \theta < \pi/2, 0 \leq \psi \leq 2\pi) \quad (14)$$

$$\Delta y = 6R_p A_{max} \Phi \sin \theta \cos \theta \sin \psi \quad (0 < \theta < \pi/2, 0 \leq \psi \leq 2\pi) \quad (15)$$

with $\Phi = \phi t$ which is the final dose or fluence of the beam. From equations (14) and (15) it is evident that the shifts in the x - y plane depend upon the electronic energy loss S_e (which enters through the parameter A_{max}), fluence Φ and the effective tilt angles θ and ψ of the beam.

The deformation yield A as a function of S_e can be written as [4]

$$A = \frac{1.16}{3e} \frac{1 + \nu}{5 - 4\nu} \frac{\beta S_e}{\rho C} \quad (16)$$

where β , ρ and C are the thermal expansion coefficient, density and specific heat capacity of the material respectively. Replacing A_{max} in equations (14) and (15) by A from equation (16) we obtain

$$\Delta x = 6R_p \Phi \frac{1.16(1 + \nu)\beta S_e}{3e(5 - 4\nu)\rho C} \sin \theta \cos \theta \cos \psi \quad (0 < \theta < \pi/2, 0 \leq \psi \leq 2\pi) \quad (17)$$

and

$$\Delta y = 6R_p \Phi \frac{1.16(1 + \nu)\beta S_e}{3e(5 - 4\nu)\rho C} \sin \theta \cos \theta \sin \psi \quad (0 < \theta < \pi/2, 0 < \psi < 2\pi). \quad (18)$$

Since the effective tilt angles θ and ψ are determined by the roughness of the surface at any instant of time during irradiation, it is very difficult to determine the values of sine and cosine of these angles. These angles keep changing during irradiation. Nevertheless, their contribution to the shift is finite and non-zero after a certain irradiation time and varies with the roughness of the surface.

3.2. Discussion

Based on the above formulism, smoothing of our samples as observed in SEM and STM can be explained. As evident from equations (17) and (18), the contribution of effective tilt angle θ to the shifts is same in x - and y -directions. However, the other tilt angle ψ gives different values to these shifts. For a real surface as shown in figure 6, the shift Δx would be larger than Δy . This would lead to a larger mass flow in the x -direction than that in the y -direction. As a result, the 'channels' (space between the 'hills') would become wider. The height of the 'hills' would decrease and the flowing mass would fill the 'valleys'.

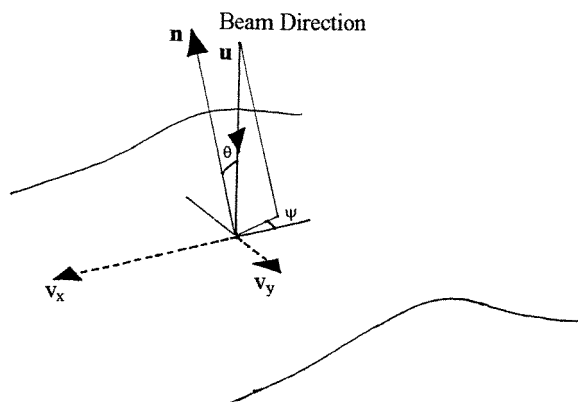


Figure 6. Schematic view of irradiation of a real (rough) surface by a normally incident beam. n represents the direction of the normal to the surface. The components of shear velocity v_x and v_y are shown by broken lines.

It is clear from equations (17) and (18) that the shifts in x - and y -directions depend upon the product of the fluence Φ and electronic energy loss S_e . Hence, to achieve the same level of surface modification at a smaller S_e , higher Φ is required. In the present work, the value of S_e was 5.75 keV nm^{-1} and therefore the smoothing was observed at a fluence two orders of magnitude higher than that in [6]. It may be concluded that the effects of small electronic energy loss ($\sim 5 \text{ keV nm}^{-1}$) together with high fluences are nearly the same as those for large electronic energy loss ($\sim 20 \text{ keV nm}^{-1}$) and comparatively low fluences. The only pronounced difference between the two situations is the formation of spherical and ellipsoidal inclusions in the former and continuous tracks in the latter case. The surface modification is not affected by the shape of inclusions in the bulk. Further work is in progress in order to understand the tilt angle dependence of shear flow and the resulting surface modifications.

Acknowledgments

This research was partially supported by UFUP grants from the Nuclear Science Centre, New Delhi. The authors are grateful to Professor S Klaumunzer for stimulating discussions related to this work during his visit to SHIMEC'98 (New Delhi, India). It is also a pleasure to thank Professor G K Mehta for his pertinent comments. Two of us at NPL (AVN and SBS) thank Professor S K Joshi for his keen interest in the work. The technical help of staff at NSC, New Delhi, during the irradiation experiments is also gratefully acknowledged.

References

- [1] Benyagaub A, Loffler S, Rammensee M, Klaumunzer S and Saemann-Ischenko G 1992 *Nucl. Instrum. Methods B* **65** 228
- [2] Klaumunzer S 1991 *Nucl. Tracks Radiat. Meas.* **19** 91
- [3] Klaumunzer S 1992 *Mater. Sci. Forum* **97-99** 623
- [4] Rao B V, Agrawal H M, Kushwaha R P S, Kanjilal D and Sharma S K 1997 *Nucl. Instrum. Methods B* **129** 487
- [5] Hou Ming-dong, Klaumunzer S and Schumacher G 1987 *Nucl. Instrum. Methods B* **19/20** 16
- [6] Guntzmann A, Klaumunzer S and Meier P 1995 *Phys. Rev. Lett.* **74** 2256
- [7] Guntzmann A and Klaumunzer S 1997 *Nucl. Instrum. Methods B* **127/128** 12
- [8] Cliche L, Rooda S, Chicoine M and Masut R A 1995 *Phys. Rev. Lett.* **75** 2348

- [9] Ziegler J F and Biersack J P 1997 *Stopping and Range of Ions in Matter* version 97.09
- [10] Trautmann C, Spohr R and Toulemonde M 1993 *Nucl. Instrum. Methods B* **83** 513
- [11] Audouard A, Mamy R, Toulemonde M, Szenes G and Thome L 1997 *Europhys. Lett.* **40** 527
- [12] Trinkaus H 1995 *J. Nucl. Mater.* **223** 196
- [13] Trinkaus H and Ryazanov A I 1995 *Phys. Rev. Lett.* **74** 5072